J|A|C|S
ARTICLES

Published on Web 05/29/2008

Evidence of an Intermediate and Parallel Pathways in Protein Unfolding from Single-Molecule Fluorescence

Angel Orte, Timothy D. Craggs,† Samuel S. White, Sophie E. Jackson,* and David Klenerman*

Department of Chemistry, University of Cambridge, Lensfield Road, Cambridge CB2 1EW, United Kingdom

Received November 5, 2007; E-mail: dk10012@cam.ac.uk; sej13@cam.ac.uk

Abstract: Determining how proteins fold into their native structures is a subject of great importance, since ultimately it will allow protein structure and function to be predicted from primary sequence data. In addition, there is now a clear link between protein unfolding and misfolding events and many disease states. However, since proteins fold over rugged, multidimensional energy landscapes, this is a challenging experimental and theoretical problem. Single-molecule fluorescence methods developed over the past decade have the potential to follow the unfolding/folding of individual molecules. Mapping out the landscape without ensemble averaging will enable the identification of intermediate states which may not be significantly populated, in addition to the presence of multiple pathways. To date, there have been only a limited number of single-molecule folding/unfolding studies under nonequilibrium conditions and no intermediates have been observed. Here, for the first time, we present a single-molecule study of the unfolding of a large autofluorescent protein, Citrine, a variant of green fluorescent protein. Single-molecule fluorescence techniques are used to directly detect an intermediate on the unfolding/folding pathway and the existence of parallel unfolding pathways. This work, and the novel methods used, shows that single-molecule fluorescence can now provide new, hitherto experimentally inaccessible, insights into the folding/unfolding of proteins.

Introduction

In the past decade, single-molecule techniques have revolutionized the information that can be obtained on complex biological systems, in addition to providing new ways of interrogating them. The ability to probe molecules one by one, free of ensemble averaging, has revealed static and dynamic heterogeneity in biological systems.[1,2] This is particularly interesting to explore the complex folding energy landscapes of proteins[3,4] or RNA molecules,[5–7] where complex conformational changes upon unfolding or misfolding can be revealed. Two distinct types of single-molecule techniques have been developed to study protein unfolding at the single-molecule level: first mechanical techniques, such as atomic force microscopy (AFM) or optical tweezers, where the force is used to unfold single proteins;[8–11] and second, unfolding of individual molecules by use of chemical denaturants[12] which is monitored by fluorescence, typically by use of fluorescence resonance energy transfer (FRET) as a "nano-ruler". Different efficiencies of energy transfer from a donor fluorophore to an acceptor dye attached in different places of the protein allowed the detection of the native and denatured conformations of small proteins such as chymotrypsin inhibitor 2 (CI2),[13–15] the cold-shock protein from *Thermotoga maritima* (Csp*Tm*),[3,16] ribonuclease H,[17–19] Im9,[20] adenylate kinase,[21] and protein A[22] under equilibrium conditions. All these studies showed typical two-state-folding behavior, and no intermediate states were detected. Frequently, a shift in the unfolded species FRET histograms has been

† Present address: School of Physics and Astronomy, University of St Andrews, North Haugh, St Andrews, Fife KY16 9SS, U.K.

(1) Haustein, E.; Schwille, P. *Curr. Opin. Struct. Biol.* **2004**, *14*, 531–540.
(2) Tinnefeld, P.; Sauer, M. *Angew. Chem., Int. Ed.* **2005**, *44*, 2642–2671.
(3) Schuler, B. *ChemPhysChem* **2005**, *6*, 1206–1220.
(4) Michalet, X.; Weiss, S.; Jager, M. *Chem. Rev.* **2006**, *106*, 1785–1813.
(5) Zhuang, X.; Bartley, L. E.; Babcock, H. P.; Russell, R.; Ha, T.; Herschlag, D.; Chu, S. *Science* **2000**, *288*, 2048–2051.
(6) Russell, R.; Zhuang, X.; Babcock, H. P.; Millett, I. S.; Doniach, S.; Chu, S.; Herschlag, D. *Proc. Natl. Acad. Sci. U.S.A.* **2002**, *99*, 155–160.
(7) Kobitski, A. Y.; Nierth, A.; Helm, M.; Jaschke, A.; Nienhaus, G. U. *Nucleic Acids Res.* **2007**, *35*, 2047–2059.
(8) Rief, M.; Gautel, M.; Oesterhelt, F.; Fernandez, J. M.; Gaub, H. E. *Science* **1997**, *276*, 1109–1112.
(9) Kellermayer, M. S. Z.; Smith, S. B.; Granzier, H. L.; Bustamante, C. *Science* **1997**, *276*, 1112–1116.
(10) Best, R. B.; Fowler, S. B.; Toca-Herrera, J. L.; Clarke, J. *Proc. Natl. Acad. Sci. U.S.A.* **2002**, *99*, 12143–12148.
(11) Fernandez, J. M.; Li, H. *Science* **2004**, *303*, 1674–1678.
(12) Tanford, C. *Adv. Protein Chem.* **1968**, *23*, 121–282.
(13) Deniz, A. A.; Laurence, T. A.; Beligere, G. S.; Dahan, M.; Martin, A. B.; Chemla, D. S.; Dawson, P. E.; Schultz, P. G.; Weiss, S. *Proc. Natl. Acad. Sci. U.S.A.* **2000**, *97*, 5179–5184.
(14) Jager, M.; Michalet, X.; Weiss, S. *Protein Sci.* **2005**, *14*, 2059–2068.
(15) Laurence, T. A.; Kong, X.; Jager, M.; Weiss, S. *Proc. Natl. Acad. Sci. U.S.A.* **2005**, *102*, 17348–17353.
(16) Schuler, B.; Lipman, E. A.; Eaton, W. A. *Nature* **2002**, *419*, 743–747.
(17) Groll, J.; Amirgoulova, E. V.; Ameringer, T.; Heyes, C. D.; Rocker, C.; Nienhaus, G. U.; Moller, M. *J. Am. Chem. Soc.* **2004**, *126*, 4234–4239.
(18) Kuzmenkina, E. V.; Heyes, C. D.; Nienhaus, G. U. *Proc. Natl. Acad. Sci. U.S.A.* **2005**, *102*, 15471–15476.
(19) Kuzmenkina, E. V.; Heyes, C. D.; Nienhaus, G. U. *J. Mol. Biol.* **2006**, *357*, 313–324.

 10.1021/ja709973m CCC: $40.75

identified as a continuum-of-substates,[19] expansion or collapse of the unfolded state,[18,23,24] or just assigned to changes in the dye's quantum yield and refractive index.[22] In some studies a clear two-state process has not been found. For instance, Mukhopadhyay et al.[25] reported a progressive expansion through a continuous ensemble of substates for the prion protein Sup35. Chirico and Baldini and co-workers[26,27] have provided evidence for several folded substates and unfolding pathways in individual GFP molecules embedded in wet nanoporous silica gels. Despite an increasing number of single-molecule unfolding studies, there have been very limited kinetic studies of folding/unfolding under nonequilibrium conditions at the single-molecule level. For instance, Kinoshita et al.[28] presented recently a technique based on a capillary flow cell to study the unfolding of single proteins, labeled with a single fluorophore. However, the only single-molecule FRET studies to date under nonequilibrium conditions using a microfluidic mixing device, performed by Eaton and co-workers[29,30] on Csp*Tm*, provided additional information on the collapsed, unfolded state of the protein. The importance of developing single-molecule techniques for the study of kinetic processes such as protein folding is shown by the fact that many proteins show classic two-state behavior under equilibrium conditions but are known to populate intermediate states under nonequilibrium conditions.[31]

In this work, we have exploited single-molecule fluorescence to explore the unfolding pathways of a large protein that is intrinsically autofluorescent, a green fluorescent protein (GFP) mutant called Citrine, under nonequilibrium conditions. Guanidinium chloride (GdmCl) was used to induce the unfolding of Citrine, a process that results in the loss of intrinsic fluorescence upon denaturation.[32] In order to facilitate the application of single-molecule fluorescence methods, an external fluorophore was covalently attached to the protein. We first studied unfolding using standard single-molecule FRET,[1] in which a single laser excites the donor molecules and both donor and acceptor fluorescence emission are detected. We also used a more sophisticated methodology, two-color coincidence detection (TCCD), which makes use of simultaneous excitation of donor and acceptor by two overlapped lasers.[33,34] This method has the advantage of being sensitive to FRET changes, as well as allowing the additional detection of fully unfolded proteins, in which the fluorescence of the intrinsic fluorophore is quenched but where there is still a signal from the attached reference dye. To make nonequilibrium single-molecule measurements, we used a nanopipette nanomixer, which we have validated previously.[35] This combination of single-molecule experiments, supported by ensemble measurements, allowed the detection and characterization of parallel unfolding pathways for Citrine, in addition to the direct detection of an intermediate state.

Materials and Methods

Citrine Preparation and Labeling. The gene encoding enhanced YFP (Clontech) was cloned into a modified pRSET vector (Invitrogen) with the C-terminal addition of a Gly-Gly spacer and a 15-residue biotinylation sequence (GLNDIFEAQKIEWHE) by polymerase chain reaction (PCR) techniques.[36] The point mutations Q69M (yielding Citrine) and E132C (providing a surface cysteine for attachment of Alexa-647; see below) were introduced by use of the QuickChange kit (Stratagene). The resulting plasmid (pCys-bio-Citrine) was fully sequenced and expressed in *Escherichia coli*. Single colonies of transformed *E. coli* cells (BL21 DE3) harboring pCys-bio-Citrine were picked from TYE ampicillin plates and used to inoculate 10 mL of 2× YT medium (containing 0.1 mg mL^{-1} ampicillin), which was then grown overnight in a shaker at 37 °C. This overnight culture was used to inoculate 1000 mL of 2× YT medium containing 0.1 mg mL^{-1} ampicillin, which was grown to a cell density (A_{600}) of 0.6−0.8 in a shaker at 37 °C. Expression of Cys-bio-Citrine was induced by the addition of isopropyl β-thiogalactoside (IPTG) to a final concentration of 0.5 mM. Expression was allowed to proceed overnight at 25 °C. Cultures were harvested by using a centrifuge (Sorvall, SLC4000 rotor, 15 min at 6000 rpm at 4 °C) and resuspended into 50 mL of lysis buffer [50 mM Tris, pH 8.0, and 1 mM tris(2-carboxyethyl)phosphine (TCEP)]. The cells were lysed by pulsed sonication on ice for 4 min and the lysate was centrifuged at 18 000 rpm (SS34, Sorvall) at 4 °C for 45 min. The supernatant was then pooled, filtered (0.22 μm syringe filter), and loaded onto a Q-Sepharose (Pharmacia) column at 2 mL min^{-1} until the yellow protein was visibly bound to the top of the column. After the column was washed for 10 column volumes (50 mM Tris, pH 8.0, 1 mM TCEP, and 100 mM NaCl), Cys-bio-Citrine was eluted with a 5 column volume salt gradient (100−300 mM NaCl) and the purity was assessed by sodium dodecyl sulfate−polyacrylamide gel electrophoresis (SDS−PAGE). The pure yellow fractions were pooled and concentrated (Vivaspins 20, Vivascience) and then loaded onto a HiLoad 26/60 Superdex G75 column (Amersham Biosciences), pre-equilibrated in buffer (50 mM Tris, pH 8.0, 1 mM TCEP, and 150 mM NaCl) and run at 3 mL min^{-1}. Two distinct yellow peaks were eluted, corresponding to monomer and a small amount of disulfide-bonded dimer. The monomer fractions were pooled and concentrated and then buffer-exchanged (PD-10 column, Amersham Biosciences) into 50 mM Tris, pH 7.1, and 1 mM TCEP. Cys-bio-Citrine was either kept in the dark at 4 °C or flash-frozen and stored at −80 °C until needed.

The commercial dye Alexa-647 (Molecular Probes) was covalently attached to the engineered cysteine residue through a thiol−maleimide linkage. The maleimide ester of Alexa-647 (1 mM) was reacted with Cys-bio-Citrine (100 μM) in the presence of TCEP (1 mM) and 50 mM Tris, pH 7.1, in a final volume of 2.5 mL. The reaction was allowed to proceed for 4 h at 25 °C in a shaker, and the reaction vessel was wrapped in foil to prevent any photochemical degradation. The only reactive Cys residue is the mutation

(20) Tezuka-Kawakami, T.; Gell, C.; Brockwell, D. J.; Radford, S. E.; Smith, D. A. *Biophys. J.* **2006**, *91*, L42–44.
(21) Rhoades, E.; Gussakovsky, E.; Haran, G. *Proc. Natl. Acad. Sci. U.S.A.* **2003**, *100*, 3197–3202.
(22) Huang, F.; Sato, S.; Sharpe, T. D.; Ying, L.; Fersht, A. R. *Proc. Natl. Acad. Sci. U.S.A.* **2007**, *104*, 123–127.
(23) Sherman, E.; Haran, G. *Proc. Natl. Acad. Sci. U.S.A.* **2006**, *103*, 11539–11543.
(24) Hoffmann, A.; Kane, A.; Nettels, D.; Hertzog, D. E.; Baumgartel, P.; Lengefeld, J.; Reichardt, G.; Horsley, D. A.; Seckler, R.; Bakajin, O.; Schuler, B. *Proc. Natl. Acad. Sci. U.S.A.* **2007**, *104*, 105–110.
(25) Mukhopadhyay, S.; Krishnan, R.; Lemke, E. A.; Lindquist, S.; Deniz, A. A. *Proc. Natl. Acad. Sci. U.S.A.* **2007**, *104*, 2649–2654.
(26) Chirico, G.; Cannone, F.; Diaspro, A. *Eur. Biophys. J.* **2006**, *35*, 663–674.
(27) Baldini, G.; Cannone, F.; Chirico, G.; Collini, M.; Campanini, B.; Bettati, S.; Mozzarelli, A. *Biophys. J.* **2007**, *92*, 1724–1731.
(28) Kinoshita, M.; Kamagata, K.; Maeda, A.; Goto, Y.; Komatsuzaki, T.; Takahashi, S. *Proc. Natl. Acad. Sci. U.S.A.* **2007**, *104*, 10453–10458.
(29) Lipman, E. A.; Schuler, B.; Bakajin, O.; Eaton, W. A. *Science* **2003**, *301*, 1233–1235.
(30) Schuler, B.; Eaton, W. A. *Curr. Opin. Struct. Biol.* **2008**, *18*, 16–26.
(31) Fersht, A. R. *Structure and Mechanism in Protein Science: Guide to Enzyme Catalysis and Protein Folding*; W.H. Freeman and Co.: New York, 1999.
(32) Fukuda, H.; Arai, M.; Kuwajima, K. *Biochemistry* **2000**, *39*, 12025–12032.
(33) Li, H. T.; Ying, L. M.; Green, J. J.; Balasubramanian, S.; Klenerman, D. *Anal. Chem.* **2003**, *75*, 1664–1670.
(34) Orte, A.; Clarke, R.; Balasubramanian, S.; Klenerman, D. *Anal. Chem.* **2006**, *78*, 7707–7715.
(35) White, S. S.; Balasubramanian, S.; Klenerman, D.; Ying, L. *Angew. Chem., Int. Ed.* **2006**, *45*, 7540–7543.
(36) Note that the biotinylation sequence was engineered into the construct for future single-molecule experiments and was not utilized in this study.

E132C, since the other two Cys present on Citrine are well buried in the folded structure. The labeled protein was separated from unreacted dye by size-exclusion chromatography (HiLoad 26/60 Superdex G75 column). The labeling efficiency was calculated to be ~35% by the absorbance method described by the dye manufacturer.

Glu132 was deemed a suitable residue for mutation and conjugation with the dye, as in the native state it is in an unstructured, solvent-exposed loop.[37] Therefore, the mutation should have little effect on the stability of the protein and, more importantly, the thiol moiety will be accessible for conjugation with the dye. Unlabeled Citrine without the E132C mutation was expressed and purified for use in the bulk studies. The E132C construct was not used as it had a tendency to form disulfide bonds.

Single-Molecule Fluorescence TCCD Coupled to Nanomixer. The instrumentation for single-molecule fluorescence TCCD and FRET has been reported in detail previously.[34] To perform TCCD measurements, both lasers were used simultaneously, whereas for FRET experiments, the same instrument was used but without excitation at 633 nm. For nanomixer experiments coupled to TCCD, a bent pipet of around 100 nm diameter is included in this confocal system (Figure 5A). Pipettes with inner radii around 50−100 nm were made with a laser-based pipet puller (Model P-2000, Sutter Instrument Co.), and bent around 45° with a gas torch. The solution was back-filled into a bent nanopipette by use of a microfiller (Microfil 34, World Precision Instruments, Sarasota, FL). A glass-bottomed dish (Willco Wells GWST 1000) containing 5 mL of buffer was used as the bath. A homemade nanomanipulation system consisting of a piezoelectric translational stage (Tritor 100, Piezosystem Jena, Germany) was used to place the nanopipette at different distances from the confocal volume and 10 μm above the dish surface. A voltage between −0.3 and −0.5 V was applied between two Ag/AgCl electrodes, one in the bath and other inside the pipet (working and ground electrodes), by use of a function generator (TG21S, Thurlby Thandar Instruments). The ion current flowing through the pipet was amplified by a high-impedance amplifier and monitored on an oscilloscope. The ion current flowing through the pipet was the same in the presence and absence of biomolecules since the ion current is dominated by the flow of sodium/potassium and chloride ions. The pipettes were loaded with 25 nM Citrine-Alx647 under native conditions (MES buffer at pH 6.0, with 0.01% Tween20 to prevent glass adhesion). In the bath, different GdmCl concentrations (6−7 M) in MES buffer with 0.01% Tween20 were used. A temperature-controlled stage (PE-94, Linkam Scientific, Surrey, U.K.) maintained a constant temperature of 25 °C throughout the experiment. The temperature was monitored by using a thermocouple microprobe (0.025-in. diameter, model 1T-1E, World Precision Instruments, Sarasota, FL) placed close to the laser focus (~1 mm), and regulated to better than ±0.2 °C. The nanomixer methodology was coupled in this work, for the first time, to the single-molecule fluorescence TCCD technique.

Single-Molecule Fluorescence TCCD and FRET Data Analysis. For FRET experiments the proximity ratio histograms of all the time bins with acceptor intensities above 10 counts ms^{-1} were analyzed (ACCEPTOR criterion). This approach filters out the zero peak, biasing the analysis to only significant FRET events. In order to build the histograms from FRET experiments, the proximity ratio is defined as

$$P = \frac{I_R}{I_B + I_R} \tag{1}$$

where I_B and I_R are the fluorescence intensities in the blue and red channels, respectively. These intensities were corrected by the background autofluorescence (0.5−1.5 kHz) and the spectral cross-talk of the blue channel into the red channel (around 1%).

For TCCD experiments, only the significant coincident events were analyzed; that is, the coincident events arising from chance were subtracted from the totals, following the methodology previously published.[34] The parameter to study the coincidence levels is the association quotient, defined as

$$Q = \frac{r_S}{r_B + r_R - r_S} = \frac{r_C - r_E}{r_B + r_R - (r_C - r_E)} \tag{2}$$

where r_S is the burst rate of the significant coincident events (chance coincident events, r_E, subtracted from the total coincident events, r_C), and r_B and r_R are the burst rates in the blue and red channels, respectively. The association quotient is proportional to the fraction of dual-labeled molecules in solution.

Unlike FRET histograms, in TCCD experiments the histograms are built from the parameter Z, given by[34]

$$Z = \ln\left(\frac{I_R}{I_B}\right) \tag{3}$$

where I_B and I_R were as defined and corrected above.

A constrained fitting procedure was used for the TCCD histograms.[38] The two populations found in Z distributions were assumed to follow Gaussian functions. The center and the widths of the Gaussians are defined by the average brightness of the blue and red fluorophores, $\langle I_B \rangle$ and $\langle I_R \rangle$, respectively. For each population, the center of the Gaussian is given by

$$x_c = \ln\left(\frac{\langle I_R \rangle}{\langle I_B \rangle}\right) \tag{4}$$

whereas the width of the Gaussian function is given by k times the shot-limited width:

$$\sigma = k\sqrt{\frac{1}{\langle I_B \rangle} + \frac{1}{\langle I_R \rangle}} \tag{5}$$

In order to constrain the fitting of the TCCD histograms from Citrine-Alx647, we assumed the brightness value of the blue fluorophore does not vary much in the two populations and this value equals the average brightness of the fluorophore during the measurement. Furthermore, the k values are known, as obtained from dsDNA model samples. The TCCD histograms showed widths between 2.2- and 2.5-fold larger than the shot-noise limited width. Therefore, only three fitting parameters are used in this model: the red fluorophore brightness values for the two populations and the relative fraction of the low-FRET species.

Results

Production of a Dye-Labeled Variant of Citrine for FRET and TCCD Measurements. We chose to study the autofluorescent protein Citrine due to its high photostability and reduced environmental sensitivity.[39,40] It differs from wild-type GFP by the point mutations S65G/V68L/Q69M/S72A/T203Y.[37] To label the protein, the mutant E132C was made in order to provide a reactive cysteine for covalent attachment of the Alexa-647 fluorophore (Figure 1). The close proximity of the Alexa-647 dye to the intrinsic fluorophore means that, upon excitation of Citrine at 488 nm, part of the energy is transferred to Alexa-647, resulting in fluorescence of the Alexa-647 (Figure 2). The FRET efficiency cannot be directly quantified from bulk experiments due to the low degree of labeling and thus the existence of a mixture of donor only and donor−acceptor

(37) Wachter, R. M.; Elsliger, M. A.; Kallio, K.; Hanson, G. T.; Remington, S. J. *Structure* **1998**, *6*, 1267–1277.
(38) Ren, X.; Li, H.; Clarke, R. W.; Alves, D. A.; Ying, L.; Klenerman, D.; Balasubramanian, S. *J. Am. Chem. Soc.* **2006**, *128*, 4992–5000.
(39) Griesbeck, O.; Baird, G. S.; Campbell, R. E.; Zacharias, D. A.; Tsien, R. Y. *J. Biol. Chem.* **2001**, *276*, 29188–29194.
(40) Shaner, N. C.; Steinbach, P. A.; Tsien, R. Y. *Nat. Methods* **2005**, *2*, 905–909.

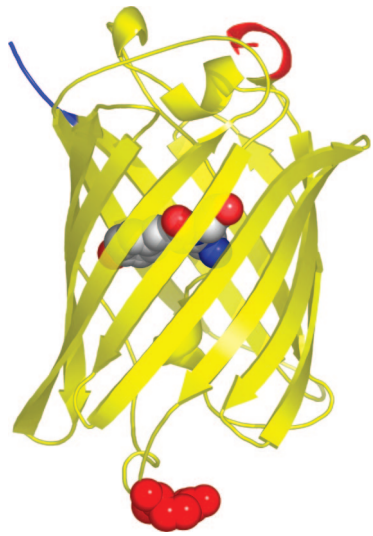

Figure 1. Ribbon diagram of Citrine (PBD code 1HUY). The N- and C-termini are shown in red and blue, respectively. The chromophore and the site of dye attachment, E132C (red), are depicted as space-filling spheres. This figure was created with PyMol (DeLano Scientific LLC).

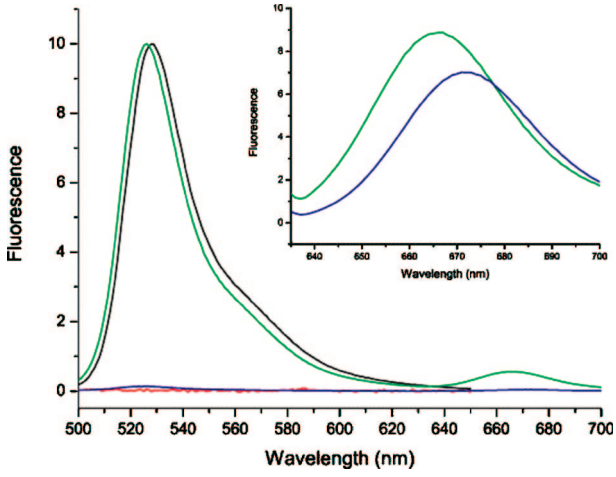

Figure 2. Emission spectra of labeled and nonlabeled proteins. Emission spectra of Citrine (native, black; denatured, red) and Citrine-647 (native, green; denatured, blue) with excitation at 488 nm (inset, excitation at 633 nm). Native spectra were obtained with 1 μM protein in 50 mM MES, pH 6.0, and 0.1 mM TCEP (denatured as for native with 6 M GdmCl). Native Citrine-647 exhibits two emission peaks, one due to its intrinsic chromophore (527 nm) and one arising from FRET to the Alexa Fluor 647 dye.

molecules. When the labeled protein was denatured in 6 M GdmCl, the Citrine fluorescence disappeared as expected, but direct excitation of the Alexa-647 showed a small shift in the emission of 10 nm and a reduction in intensity of only 25% due to the change in solvent conditions (Figure 2). This indicated that Alexa-647 stayed fluorescent under these conditions and could be used to report back on the conformation of the Citrine via FRET with the Citrine chromophore.

Single-Molecule FRET and TCCD Measurements under Native Conditions. Initial single-molecule FRET experiments were performed on the Alexa-647-labeled Citrine (Citrine-Alx647) under native conditions at 0 M GdmCl. In order to build up histograms from the single-molecule data, a proximity ratio is used. This is a measure of the relative intensity of the acceptor emission divided by the total emission from acceptor and donor, see Materials and Methods for more details. A high proximity ratio is indicative of effective energy transfer and

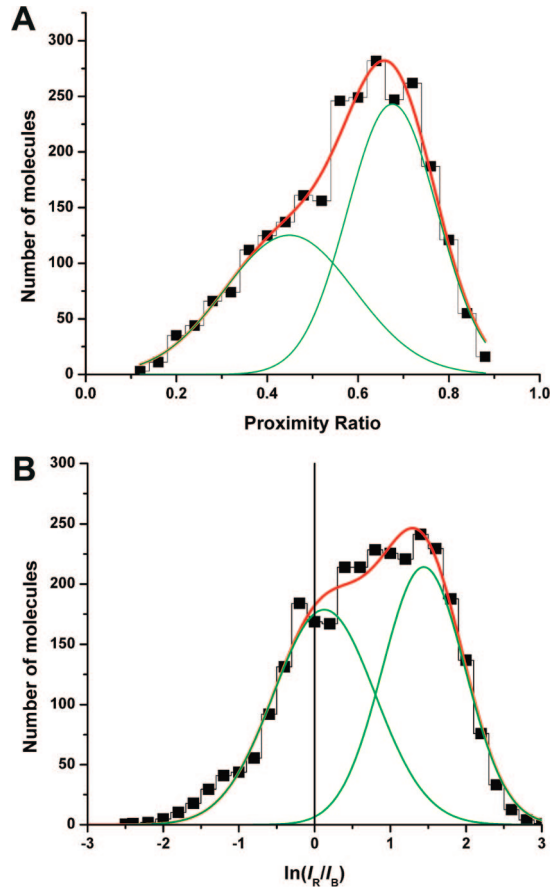

Figure 3. Single-molecule histograms of labeled Citrine in native conditions. (A) Proximity ratio histogram from a FRET measurement (only donor excitation), fitted with two Gaussian peaks centered at 0.45 and 0.68. (B) *Z* function histogram from a TCCD measurement, fitted with two Gaussian peaks centered at 1.44 and 0.13.

thus close proximity of acceptor and donor chromophores as expected in the native state. For Citrine, the proximity ratio of the denatured state is zero, as the intrinsic yellow chromophore loses fluorescence on denaturation and no FRET can occur. The histograms from the single-molecule data acquired under native conditions are shown in Figure 3A. Two peaks were observed in these experiments and the histogram produced was fitted with a high proximity subpopulation at 0.68 and a lower proximity subpopulation at 0.45 (Figure 3A), suggesting the presence of an additional species with a lower FRET efficiency than the native state.

FRET histograms follow Gaussian functions only approximately,[41] and therefore to avoid possible artifacts or false populations due to deviations from a normal distribution, TCCD was used.[33,34] This approach has the advantage that there is an easily determinable optimum single criterion to detect coincidence bursts. We formed histograms of Z, defined as $\ln(I_R/I_B)$, where I_R and I_B are the fluorescence intensities of the bursts in the red and blue channels, respectively. The distributions of Z follow a normal distribution, since direct ratios (like I_R/I_B) are known to fit to log-normal distributions.[42] Figure 3B shows the result of a TCCD experiment on the labeled Citrine under native conditions. Again, we detected two clear subpopulations in the

(41) Ying, L.; Wallace, M. I.; Balasubramanian, S.; Klenerman, D. *J. Phys. Chem. B* **2000**, *104*, 5171–5178.
(42) Limpert, E.; Stahel, W.; Abbt, M. *Bioscience* **2001**, *51*, 341–352.

histograms of Z, with Z values around 1.4 ($I_R/I_B \sim 4.1$), indicating a high FRET population, and a second peak centered around 0.1 ($I_R/I_B \sim 1.1$) indicating a lower FRET population which, on average, accounted for approximately 26% of the total.[43]

In order to rule out that this dual-peak histogram was an artifact of TCCD applied to systems showing FRET, we also measured a control, which was a 40 base-pair length of double-stranded DNA, dual-labeled with Alexa-488 and Alexa-647 dyes separated by 10 base pairs. This control shows a FRET peak, in proximity ratio histograms, centered at similar values to our Citrine-Alx647. When this sample was measured with TCCD, unlike the Citrine-Alx647, only a single Gaussian-like peak with a Z value around 1.4 was observed (Figure 1 in Supporting Information). Thus, using both single-molecule FRET and TCCD we detect the presence of two structured states under equilibrium conditions for Citrine-Alx647. We also ruled out the possibility that the two peaks arise from photophysical effects by studying the effect of laser power on TCCD histograms and autocorrelation functions (see Figures 2 and 3 in Supporting Information). In addition, the excited-state protonation of the Citrine chromophore is not the cause of the low-FRET population since it is a dark state[44] unable to give rise to FRET. If there is dynamic interconversion between the two FRET states, it must occur on a time scale longer than the diffusion time across the probe volume, 300 μs, significantly slower than the rate of protonation/deprotonation (see Discussion 1 in Supporting Information).

Equilibrium Measurements on Citrine Unfolding. An equilibrium unfolding experiment was performed on the Alexa-647-labeled Citrine by use of single-molecule TCCD and FRET. As it is now clearly established that the unfolding of the close homologue of Citrine, green fluorescent protein (GFP), is slow at low concentrations of denaturant and therefore the protein takes some time to reach its true equilibrium in an unfolding titration,[45,46] samples were left to incubate for 144 h before measurements were made. For both techniques, a biphasic unfolding transition was observed (Figure 4A), suggesting the population of an intermediate state even under equilibrium conditions. The population of the two states determined by TCCD varied with GdmCl concentration (Figure 4B) with an increasing relative population of the low-FRET species at GdmCl concentrations above 1 M. This suggests that the high-FRET species may unfold via the low-FRET state. The equilibrium is shifted to a higher population of low-FRET species with increasing GdmCl concentration.

In order to establish that these results were not an artifact of the single-molecule measurements, or the covalent modification of the protein with dye, an equilibrium unfolding curve for unlabeled Citrine was also monitored by Citrine fluorescence

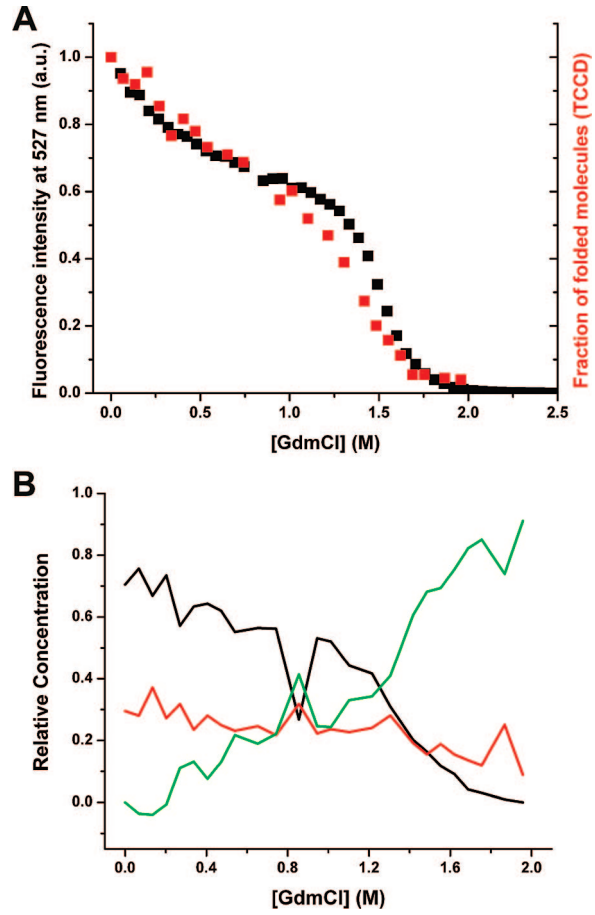

Figure 4. Equilibrium unfolding curves of Citrine. (A) Normalized equilibrium unfolding curves for Citrine obtained by ensemble fluorescence (black symbols, fluorescence at 527 nm) and for Citrine-Alx647 obtained by TCCD (red symbols, association quotient), after 144 h of incubation. Error bars for TCCD measurements are lower than ± 0.04. (B) Relative populations of the high-FRET (black) and low-FRET (red) substates and the unfolded state (green) from the TCCD equilibrium experiments of 50 pM Citrine-Alx647 incubated for 144 h at increasing GdmCl concentrations.

(527 nm) in a bulk mode (Figure 4A). Note that the fluorescence spectrum showed a change in intensity but no spectral shifts upon addition of GdmCl (data not shown). The curve was also biphasic and within experimental error of those obtained by single-molecule TCCD or FRET, suggesting a partially structured intermediate state is populated for Citrine and this is an intrinsic property of the protein. In fact, it has recently been shown that GFP populates an intermediate state under equilibrium conditions,;[45,46] however, it does appear from these results that the native state of Citrine is significantly less stable than that of GFP.

Global fitting of the bulk measurement data to a three-state model gave a good fit (Figure 4 in Supporting Information), and from this fit structural parameters were obtained. The value for the fluorescence of the intermediate state was $S_I = 60\% \pm 5\%$ (quoted as a percentage with reference to the native state signal). By use of the m values also obtained from the fit, which are proportional to the change in solvent-accessible surface area (SASA) of the residues in a protein upon a change in conformation, the relative compactness of the intermediate state could be estimated: the value was 0.59 ± 0.05, indicating that some 60% of the surface area buried in the native state is buried in the intermediate. The relative instability of the native state

(43) Note that there is a correction factor for the relative populations of the two FRET states due to different detection efficiencies on TCCD for different FRET values. Higher FRET values give rise to lower detection efficiencies. Using model DNA samples with FRET efficiencies of 0.8 and 0.5 we have determined a correction factor of 1.88 for the population of the highFRET species respect to the lowFRET. The details of this study will be published elsewhere. From the fit of YFP-Alx647 histograms, the average lowFRET fraction was 0.4, and is then converted into 0.26 by applying this correction factor.

(44) Heikal, A. A.; Hess, S. T.; Baird, G. S.; Tsien, R. Y.; Webb, W. W. *Proc. Natl. Acad. Sci. U.S.A.* **2000**, *97*, 11996–12001.
(45) Huang, J.-R.; Craggs, T. D.; Christodoulou, J.; Jackson, S. E. *J. Mol. Biol.* **2007**, *370*, 356–371.
(46) Andrews, B. T.; Schoenfish, A. R.; Roy, M.; Waldo, G.; Jennings, P. A. *J. Mol. Biol.* **2007**, *373*, 476–490.

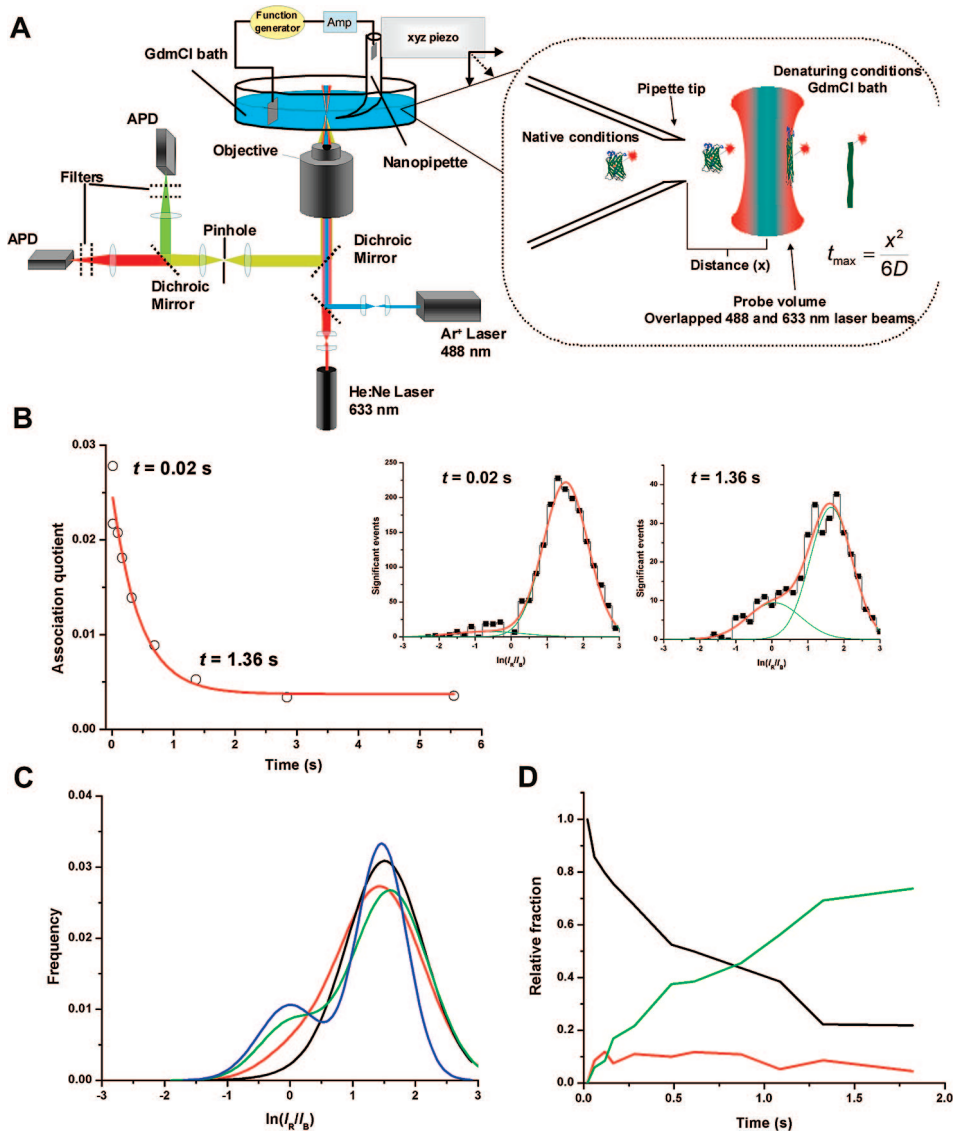

Figure 5. Unfolding of labeled Citrine studied by TCCD/nanomixer. (A) Schematic of the TCCD coupled to a 100 nm diameter glass pipet and basics of the nanomixer methodology. (B) Typical unfolding curve obtained in the TCCD-nanomixer experiments (6.6 M GdmCl), showing the time decay of the association quotient. The *Z* distributions and fitting functions at the times of 0.02 and 1.36 s are also shown. (C) Normalized TCCD histograms fitting functions after 0.02 (black), 0.69 (red), 1.36 (green), and 2.84 (blue) s. (D) Relative populations of the high-FRET (black) and low-FRET (red) substates and the unfolded state (green).

of Citrine with respect to the intermediate state, compared with GFP, can be seen by comparing the free energy changes associated with the transition from native (N) to intermediate (I) (ΔG_{N-I}) and intermediate to denatured (D) states (ΔG_{I-D}). The values are 1.2 and 6.0 kcal mol^{-1} for ΔG_{N-I} and 7.6 and 10.5 kcal mol^{-1} for ΔG_{I-D} for Citrine and GFP, respectively. Thus, from the results obtained for Citrine, one expects some 10−20% of the protein to be in the intermediate state even in the absence of denaturant.

Single-Molecule Unfolding Kinetics. Unfolding studies at the single-molecule level were then undertaken over a wide range of denaturant concentrations by combining manual mixing experiments for the slow unfolding observed at low GdmCl concentrations with a nanopipette-based nanomixer for fast unfolding at higher GdmCl concentrations (above 5.5 M). The nanomixer allows the study of fast reaction kinetics at the single-molecule level,[35] otherwise not accessible. The nanomixer is built up by a 100 nm inner diameter glass pipet, which is introduced into a confocal system (Figure 5A). The protein is loaded under native conditions inside the pipet, and a moderate voltage applied between the electrodes drives the molecules to the pipet tip by a combination of electrophoretic, dielectrophoretic, and electro-osmotic forces.[35,47] Once the molecules leave the pipet tip, they diffuse into the denaturing buffer bath, and changes in conformation are explored by probing with the focused laser at different distances away from the tip by TCCD. The advantage of using TCCD is that it allows the detection of both the folded and unfolded species. Figure 5A shows the basics of the nanomixer measurements on Citrine-Alx647 unfolding. The distance (from probe volume to tip), x, can be transformed into the most probable time, t_{max} that the molecules have diffused in the denaturing buffer until detection by use of the three-dimensional diffusion equation:

$$t_{max} = x^2/6D \qquad (6)$$

where D is the diffusion coefficient of the molecule.[35] Because the diffusion coefficients are different for folded and unfolded Citrine, the use of this equation is not straightforward. We have

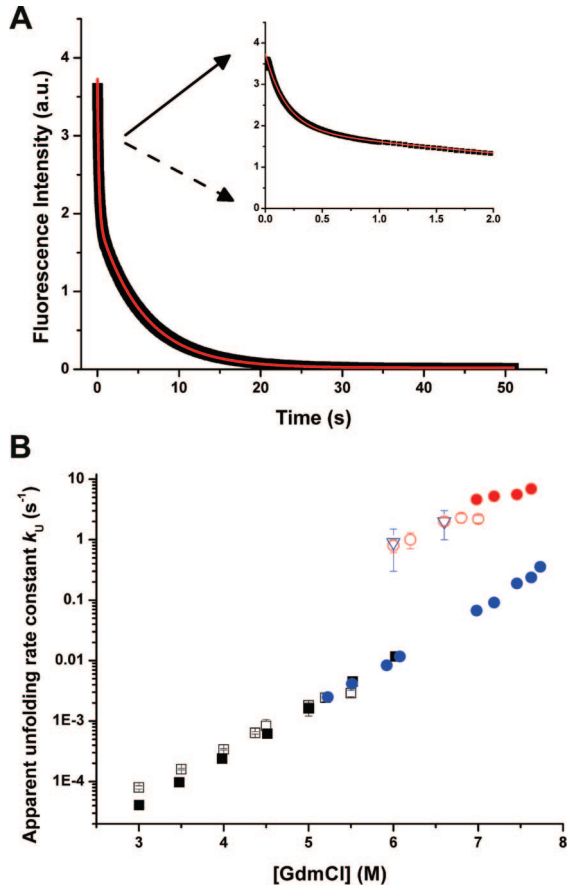

Figure 6. Measured average values ofk_U at different GdmCl concentrations. (A) Unfolding fluorescence decay trace from a stopped-flow measurement (6.9 M GdmCl). A double-exponential function (red line) was used to fit the experimental data. The inset shows the first 2 s of the decay. (B) Average unfolding rate constants from different techniques: ensemble measurements in solution (■), FRET in solution (□), TCCD/nanomixer in continuous mode (○, red), and TCCD/nanomixer in pulsed-gated mode (▽, blue). The stopped-flow experiments showed biexponential decays above 6 M GdmCl, and thus a fast (●, red) and a slow rate (●, blue). Error bars show ±1 SD of the average value.

corrected for this using an average weighted diffusion coefficient (see Discussion 2, Table 1, and Figures 5 and 6 in Supporting Information). The actual arrival time of the molecule to the probe volume may vary from that obtained by eq 6 due to an effective distribution of diffusion trajectories. However, the use of the most probable time should average out this effect. Indeed, the arrival of folded molecules with $t < t_{max}$ would be compensated by the detection of later (probably unfolded) molecules with $t > t_{max}$. Therefore, we have validated this approach by operating the nanomixer in a pulsed mode, where the time to the detection volume is measured directly (detailed in Discussions 3 and 4 and Figures 7−9 in Supporting Information). Figure 5B shows a typical decay of association quotient, proportional to the fraction of folded molecules, with time obtained in a TCCD-nanomixer experiment, and the TCCD histograms associated with two different time points.

Figure 5C shows the TCCD histograms obtained at different times after the folded Citrine leaves the tip of the nanopipette and diffuses into a bath of 6.6 M GdmCl. Initially, there is only a high FRET subpopulation detectable, so the Citrine is not under equilibrium conditions when it exits the pipet. This is possibly due to preunfolding of the low-FRET peak promoted by the high electric field at the pipet tip, similar to results observed previously with GFP[48] (see Discussion 5 and Figure 10 in Supporting Information). However, after 0.69 s the low-FRET peak has clearly appeared in the histogram. Figure 5D shows the normalized concentration profiles of the high-FRET, low-FRET, and unfolded species upon the diffusion of the molecules out of the nanopipette into a 6.6 M GdmCl bath. This clearly demonstrates some buildup of a steady population of the low-FRET subpopulation as the Citrine unfolds. This suggests that one path to the unfolded Citrine is for the high-FRET subpopulation to interconvert with the low-FRET population.

The rate of unfolding of the unlabeled protein was then measured via bulk techniques, manual mixing and stopped-flow, as a function of GdmCl concentration between 3 and 7.7 M. Unfolding was followed by the loss of yellow fluorescence (excitation 488 nm, emission 527 nm). Below 6.9 M the decay was fitted with a single exponential, but for higher concentrations of denaturant a single exponential was insufficient, and clear biexponential behavior was found (with a decrease in the χ^2 value of 2 orders of magnitude; see Figure 11 in Supporting Information), as shown in Figure 6A. These experiments together suggest the presence of an intermediate state of decreased brightness in the unfolding of Citrine.

Finally, Figure 6B shows the rate constants obtained for both the ensemble and single-molecule measurements: manual mixing, stopped-flow, and nanomixer experiments. The slow decay observed in the bulk stopped-flow measurements is in good agreement with the rates obtained in the single-molecule FRET and TCCD experiments. The fast decay from the stopped-flow experiment agrees well with the rates obtained in the single-molecule nanomixer experiments.

Kinetic Schemes. There is clear evidence from both the single-molecule and ensemble measurements presented here that an intermediate state is populated during the unfolding of Citrine. Our results suggest the kinetic scheme for Citrine-Alx647 unfolding shown in Scheme 1, where the low-FRET and high-FRET coexist under native conditions. The simplest model, in which the native state unfolds via an on-pathway intermediate state to the denatured state, N ⇆ I ⇆ D, where N is the high-FRET subpopulation and I is the low-FRET population, turns out to be insufficient to explain all our observations. Instead, a triangular kinetic model (Scheme 1) more accurately fits the data, and explains the overall behavior of the unfolding of the labeled protein. In this model, there are parallel unfolding pathways: in one of which Citrine unfolds via the intermediate low-FRET state, while in the other there is a direct conversion of native Citrine to the denatured state. The validity of the kinetic model was tested by simulations, by deriving the equations that predict the concentration profiles of each species with time. These equations are detailed in Discussion 6 in Supporting Information. Some simplifications to the kinetic scheme can be made under certain experimental conditions, as shown in Scheme 1. For instance, under strongly denaturing conditions, we assume k_{hl} to be negligible (Scheme 1C). This is based on considering the low-FRET species to be an on-pathway intermediate, as suggested by experimental evidence, because it is unlikely that the intermediate refolds to the native state under these conditions. This is indeed the situation in the nanomixer and stopped-flow unfolding experiments. We can simulate the

(47) Ying, L.; White, S. S.; Bruckbauer, A.; Meadows, L.; Korchev, Y. E.; Klenerman, D. *Biophys. J.* **2004**, *86*, 1018–1027.

(48) Baldini, G.; Cannone, F.; Chirico, G. *Science* **2005**, *309*, 1096–1100.

Scheme 1. Proposed Triangular Kinetic Scheme for Citrine-Alx647 Unfolding under Different Experimental Conditions[a]

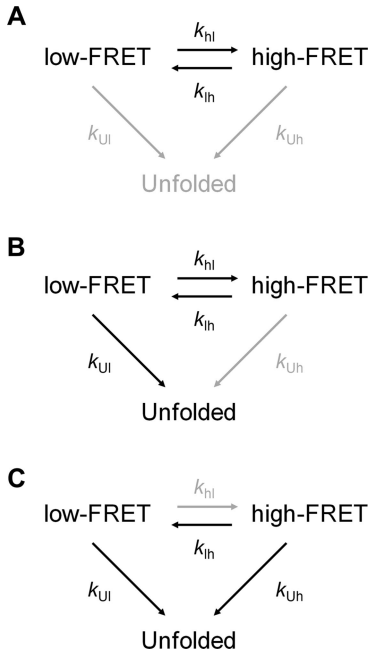

[a] (A) Native and (B) unfolding conditions at moderate [GdmCl], and (C) unfolding conditions at high [GdmCl]. k_{hl} and k_{lh} are the rate constants for the interconversion of the high- and low-FRET species, and k_{Ul} and k_{Uh} are the rate constants for the unfolding of the low- and high-FRET species to the denatured state, respectively.

concentration profiles of the high-FRET, low-FRET, and unfolded species and compare them to experimental data. Figure 7A shows the experimental concentration profiles from a nanomixer experiment at 6.6 M GdmCl, along with the simulated curves. From these simulations, we can also obtain the fraction of dual-labeled molecules, that is, the overall fraction of folded proteins. This fraction is proportional to the parameter of interest in TCCD-nanomixer experiments, the association quotient (eq 2). Figure 7B shows the good agreement between the normalized experimental association quotient obtained in the 6.6 M GdmCl experiment and the simulated curve of fraction of folded proteins. Interestingly, through these simulations we ruled out the possibility of a single unfolding pathway through the intermediate state, that is, the simple consecutive reactions scheme. Indeed, the marked decrease in the association quotient on the nanomixer experiments can be explained only if a direct unfolding reaction of the high-FRET species is possible (see Discussion 6 and Figures 12−15 in Supporting Information for details). In contrast, in the experiments at moderate GdmCl concentrations with manual mixing, it is the equilibrium between the high-FRET and low-FRET species that controls the unfolding behavior, and the approximation of k_{hl} being negligible is no longer valid. As shown in Scheme 1B, the results at moderate GdmCl concentrations can be explained through a sequential model where the equilibrium between the native and intermediate species is the main reaction taking place (see Discussion 6 in Supporting Information).

Discussion

Although single-molecule techniques are fast becoming established in many areas of science, particularly in biological sciences, almost all the studies that have been performed so far have been on systems at equilibrium. While this has provided

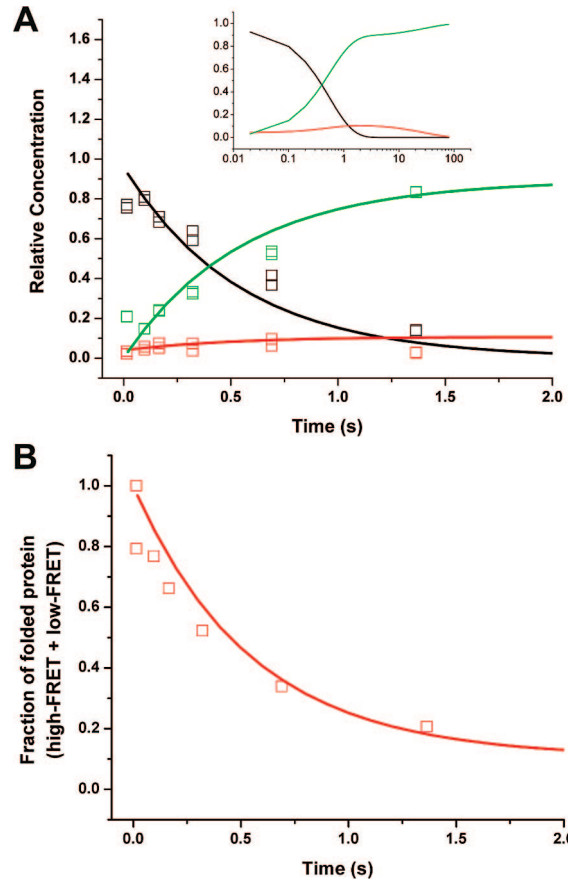

Figure 7. Simulations from the kinetic model for Citrine-647 unfolding scheme and comparisons with experimental data. (A) Experimental (symbols) and simulated (lines) relative populations of the high-FRET (black) and low-FRET (red) substates and the unfolded state (green) upon unfolding in 6.6 M GdmCl. The simulation was performed with the following parameters: $k_{lh} = 0.14\ s^{-1}$, $k_{Uh} = 1.697\ s^{-1}$, $k_{Ul} = 0.0338\ s^{-1}$, $k_{hl} = 0$, and $f_0 = 0.04$, fulfilling the experimental overall rate constants $k_1 = -\gamma_1 = 0.0338\ s^{-1}$ and $k_2 = -\gamma_2 = 1.837\ s^{-1}$. (B) Experimental normalized association quotient (symbols) and simulated fraction of folded protein (line) upon unfolding in 6.6 M GdmCl.

a wealth of important information on the conformational dynamics of the native and denatured states of proteins, it has limited the application of single-molecule methods for studying what are thought to be very complex energy landscapes such as those for protein folding. The Eaton group is one of the few that have studied protein folding reactions using single-molecule approaches with a microfabricated laminar-flow mixer in conjunction with a confocal optical system. In their FRET-based system, the folding of the small protein Csp*Tm* was investigated; however, no subpopulations were observed but important information on the nature of the denatured ensemble was obtained.[29]

Here, we present a new method for the single-molecule measurement of protein unfolding and folding processes, which we have applied to the study of the unfolding pathway of the large β-barrel protein Citrine. By use of a dye-labeled variant of Citrine, two different and complementary experimental methods were employed to probe the state of the protein during the unfolding reaction: a FRET-based assay detecting energy transfer between the intrinsic yellow chromophore of Citrine and an attached acceptor dye, and TCCD, in which both the yellow chromophore and the covalently attached Alexa-647 are monitored during unfolding, the yellow chromophore acting as a sensitive probe of the state of the protein.

Our results showed that even under native conditions Citrine populates two states: one has a high FRET efficiency, and the other has a lower FRET signal. There is good evidence that this low-FRET species is a partially structured intermediate state of Citrine and not either a conformational substate of the native state or an artifact of the dye labeling of the protein or the single-molecule measurements. First, Citrine and Citrine labeled with Alexa-647 give similar equilibrium curves. Second, two states of Citrine were previously observed in fluorescence lifetime measurements with lifetimes of 3.31 and 0.88 ns.[44] If the longer lifetime is assigned to the folded state, then the existence of a second state, with reduced quantum yield, would lead to reduced FRET in the presence of the Alexa-647 acceptor. The two FRET states we observe are in good agreement with this prediction, indicating that the dominant contribution to the FRET changes we observe are changes in donor quantum yield rather than donor−acceptor separation (Discussion 7 and Figure 16 in Supporting Information). Third, these measurements are made with very dilute solutions of proteins so that dimerization of the protein can be ruled out. GFP has been shown to dimerize only at very high concentrations, the dimerization constant being estimated at 60 μM.[49,50] Fourth, filtered ratiometric fluorescence correlation spectroscopy (FCS) showed a power-independent fast protonation of the Citrine to its neutral state. Since the neutral state is dark and the protonation rate is very fast, this protonation is not responsible for the appearance of a second low-FRET peak in the single-molecule histograms. Finally, and most importantly, we have directly observed just the folded state at early times in the nanomixer experiment and subsequently observed the appearance of the intermediate FRET state after longer times, as the folded state decreases. If the states we observe were formed by a photophysical reaction in the excited state of Citrine, then we would have observed both states at early times. Our results directly rule out photophysics in the excited state contributing to the results and indicate that the two FRET states detected are directly reporting back about states of the ground-state protein.

In addition to the data presented here, there is increasing experimental and computational evidence from other studies that GFP and its variants populate a partially structured intermediate.[45,46,51,52] Both our own group and the Kuwajima group have identified an intermediate state in which it is speculated that three or four β-strands of the β-barrel have unraveled, partially exposing the central chromophore. A comparison of the thermodynamic parameters obtained for the GdmCl-induced unfolding of GFPuv to those measured here for Citrine indicate that a similar degree of structure has been lost in the intermediate state in both cases (the β-Tanford value for the intermediate state, which is a measure of the amount of solvent-accessible surface area buried in the intermediate state relative to the native state, is 0.59 for Citrine in comparison to 0.62 for GFPuv). In contrast to the similarity between the *m* values for Citrine and GFPuv, which report on global changes in solvent-accessible surface area, the free energy differences between the native, intermediate, and denatured states are quite different for the two proteins. In particular, the native state of Citrine is relatively unstable with respect to the intermediate state with a ΔG_{N-I} of 1.2 kcal mol^{-1} compared to 6.0 kcal mol^{-1} for GFPuv. It is, therefore, not surprising that we observe the intermediate state of Citrine even under native conditions. The intermediate state of Citrine also appears to be destabilized with respect to the denatured state when compared with GFPuv, however, not to the same extent as observed for the native−intermediate transition. The values for ΔG_{I-D} are 7.6 and 10.5 kcal mol^{-1} for Citrine and GFPuv, respectively. It is hard to attribute these changes in energy to specific mutations in the protein as there are many differences between GFPuv and Citrine. Many of the mutations in Citrine (including S65G, V68L, Q69M, and S72A) are located in the central α-helix that runs through the core of the β-barrel structure, and along with T203Y the side chains of these residues are all buried. Mutation of any of them could disrupt stability of the native and/or intermediate state.

Kinetic, single-molecule studies of the unfolding of Citrine were also undertaken over a wide range of chemical denaturant concentrations to probe the energy landscape of folding further. TCCD experiments revealed that the low-FRET species observed in the equilibrium studies was also observed during the unfolding of Citrine, suggesting that it may be an on-pathway intermediate. By a careful analysis of the single-molecule unfolding data acquired at low and high concentrations of denaturant, it was possible to establish that Citrine unfolds through two parallel pathways, one of which involves the low-FRET state while the other involves the direct conversion of the native state to the denatured state, under the conditions used (Scheme 1). The scheme was consistent with the bulk unfolding measurements, which at high concentrations of denaturant show two unfolding phases, one attributable to unfolding of the low-FRET species.

There have been a number of studies on the unfolding kinetics of GFP and its variants, most of them using ensemble measurements of fluorescence. It is a little difficult to carry out a direct comparison of these results with those presented here, as conditions and protein constructs used in the different studies are highly variable. For example, studies by the Winter group[53] used pressure to induce unfolding of red-shifted GFP. In this case, although a simple single-exponential process was observed, there was evidence that there may be more than one pathway to unfolding as the relaxation constants measured were dependent upon the direction of the pressure jump. Work published by the Kuwajima group[54] on the cycle3 mutant of GFP used acid to induce unfolding and the kinetics were found to be highly dependent upon pH. In conjunction with refolding measurements, a kinetic scheme was proposed in which there are two molten globule-like intermediate states populated late on the folding pathway, both of which fold to the native structure,[54] suggesting that there would be two unfolding pathways consistent with our data.

Several groups have used guanidinium chloride to induce unfolding and study the unfolding kinetics. In the first study, the kinetics of GdmCl-induced unfolding of a range of monomeric and oligomeric fluorescent proteins (FPs) was undertaken to measure the relative stabilities of monomeric, dimeric, and

(49) Wiehler, J.; Jung, G.; Seebacher, C.; Zumbusch, A.; Steipe, B. *ChemBioChem* **2003**, *4*, 1164–1171.
(50) Jung, G.; Ma, Y.; Prall, B. S.; Fleming, G. R. *ChemPhysChem* **2005**, *6*, 1628–1632.
(51) Helms, V.; Straatsma, T. P.; McCammon, J. A. *J. Phys. Chem. B* **1999**, *103*, 3263–3269.
(52) Enoki, S.; Maki, K.; Inobe, T.; Takahashi, K.; Kamagata, K.; Oroguchi, T.; Nakatani, H.; Tomoyori, K.; Kuwajima, K. *J. Mol. Biol.* **2006**, *361*, 969–982.
(53) Herberhold, H.; Marchal, S.; Lange, R.; Scheyhing, C. H.; Vogel, R. F.; Winter, R. *J. Mol. Biol.* **2003**, *330*, 1153–1164.
(54) Enoki, S.; Saeki, K.; Maki, K.; Kuwajima, K. *Biochemistry* **2004**, *43*, 14238–14248.

tetrameric FPs.[55] In this case, however, monoexponential kinetics were observed and the data were not analyzed in detail, nor was a kinetic scheme proposed. In a more recent study, the Jennings group[46] have also studied the GdmCl unfolding kinetics of GFP and observed that the reaction has at least two exponential components, consistent with our observations on Citrine. All of these studies used bulk measurements of fluorescence or some other probe; however, a single-molecule study on the unfolding of a variant of GFP, GFPmut2, has been published.[27] In this study, the proteins were encapsulated in wet silica gels and the switching rate between different states of GFPmut2 with different photophyscial properties was used to inform on the conformational heterogeneity of the system: several substates of the apparently "native" protein were observed. Under denaturing conditions, the switching rate displayed different and reproducible time evolutions, suggesting that the various conformational substates unfold along separate pathways. This is consistent with our results, which show that there are parallel pathways to unfolding. Whether one of the conformational substates observed in this study is the same as the low-FRET intermediate state shown here remains to be established.

The studies described above, together with our single-molecule study, clearly show that the unfolding behavior of Citrine/GFP is complex, that at least one intermediate state is populated during unfolding, and that the protein can unfold along multiple pathways. Single-molecule studies will play an important role in elucidating more of the features of the folding energy landscape of this important class of protein.

Conclusions

We have used a combination of bulk and single-molecule fluorescence methods to probe the unfolding of Citrine, which give consistent results and provide direct evidence for a populated substate, which is on-pathway on the unfolding/folding energy landscape. This is the first time a protein unfolding intermediate has been directly identified by single-molecule fluorescence methods. In addition, we have identified two distinct conformations from which the protein unfolds along parallel pathways. From our previous results of H/D exchange NMR studies on GFP,[45] we have proposed a structure for this intermediate, in which β-strands 7−10 are partially unfolded, with the rest of the β-barrel structure remaining intact. This partially open structure would increase the accessibility of the solvent to the Citrine chromophore, allowing quenching and lowering the donor quantum yield. As a consequence the FRET efficiency is reduced.

This work demonstrates that single-molecule fluorescence methods have now reached a stage where they can start to probe the details of protein folding/unfolding mechanisms and directly detect the presence of intermediate states on the energy landscape, even those that may not be significantly populated. Although the method employed here was to use FRET between the intrinsic Citrine chromophore and a covalently attached dye, having now established this powerful methodology, these methods can be extended to many other systems by the double-labeling of proteins with suitable donor−acceptor FRET pairs.[56] This paves the way for detailed single-molecule studies on protein folding pathways that can be used to address some of the major issues in the field. Ultimately, this will allow the direct comparison of experimental data from single-molecule studies with computational work performed on the level of individual polypeptide chains.

Acknowledgment. We thank L. Ying for comments and his involvement in the early stage of the project and A. Bruckbauer for helpful discussions. This work was supported by grants from the BBRSC (T.D.C., S.S.W., S.E.J., and D.K.) and the 6th Framework Marie Curie EIF (A.O.).

Supporting Information Available: Detailed description of additional methods; additional figures, discussions, and references. This material is available free of charge via the Internet at http://pubs.acs.org.

JA709973M

(55) Stepanenko, O. V.; Verkhusha, V. V.; Kazakov, V. I.; Shavlovsky, M. M.; Kuznetsova, I. M.; Uversky, V. N.; Turoverov, K. K. *Biochemistry* **2004**, *43*, 14913–14923.

(56) Merchant, K. A.; Best, R. B.; Louis, J. M.; Gopich, I. V.; Eaton, W. A. *Proc. Natl. Acad. Sci. U.S.A.* **2007**, *104*, 1528–1533.